


Methyl arachidonyl fluorophosphonate inhibits *Mycobacterium tuberculosis* thioesterase TesA and globally affects vancomycin susceptibility

Dong Yang¹, Guy Vandebussche² , Didier Vertommen³, Damien Evrard⁴, Romany Abskharon^{5,6}, Jean-François Cavalier⁷, Gilles Berger¹, Stéphane Canaan⁷, Mohammad Shahneawz Khan⁴, Sheng Zeng¹, Alexandre Wohlkönig⁶, Martine Prévost², Patrice Soumillion⁴ and Véronique Fontaine¹ 

- 1 Microbiology, Bioorganic and Macromolecular Chemistry Unit, Faculty of Pharmacy, Université Libre de Bruxelles (ULB), Belgium
 2 Laboratory for the Structure and Function of Biological Membranes, Faculty of Sciences, Université Libre de Bruxelles (ULB), Belgium
 3 de Duve Institute, Université Catholique de Louvain (UCL), Brussels, Belgium
 4 Biochemistry and Genetics of Microorganisms, Louvain Institute of Biomolecular Science and Technology, Université Catholique de Louvain (UCL), Louvain-la-Neuve, Belgium
 5 National Institute of Oceanography and Fisheries (NIOF), Cairo, Egypt
 6 VIB-VUB Center for Structural Biology, Vrije Universiteit Brussel (VUB), Brussels, Belgium
 7 CNRS, LISM, IMM FR3479, Aix-Marseille University, France

Correspondence

V. Fontaine, Microbiology, Bioorganic and Macromolecular Chemistry Unit, Faculty of Pharmacy, Université Libre de Bruxelles (ULB), Boulevard du Triomphe, CP205/2, 1050 Brussels, Belgium
 Tel: +32 (0)2 650 52 96
 E-mail: vfontain@ulb.ac.be

Guy Vandebussche, Patrice Soumillion and Véronique Fontaine contributed equally to this research

(Received 17 May 2019, revised 18 July 2019, accepted 25 July 2019, available online 28 August 2019)

doi:10.1002/1873-3468.13555

Edited by Peter Brzezinski

Phthiocerol dimycocerosates and phenolic glycolipids (PGL) are considered as major virulence elements of *Mycobacterium tuberculosis*, in particular because of their involvement in cell wall impermeability and drug resistance. The biosynthesis of these waxy lipids involves multiple enzymes, including thioesterase A (TesA). We observed that purified recombinant *M. tuberculosis* TesA is able to dimerize in the presence of palmitoyl-CoA and our 3D structure model of TesA with this acyl-CoA suggests hydrophobic interaction requirement for dimerization. Furthermore, we identified that methyl arachidonyl fluorophosphonate, which inhibits TesA by covalently modifying the catalytic serine, also displays a synergistic antimicrobial activity with vancomycin further warranting the development of TesA inhibitors as valuable antituberculous drug candidates.

Keywords: methyl arachidonyl fluorophosphonate; *Mycobacterium tuberculosis*; TesA; tetrahydrolipstatin; vancomycin

Mycobacterium tuberculosis is the causative agent of tuberculosis (TB), a life-threatening disease representing a major global health burden. Globally, an estimated 10.0 million people contracted TB in 2017 and 558 000 TB cases were resistant to rifampin, one of

the first-line antituberculous drugs [1]. Among these resistant strains, more than 80% were multidrug-resistant (MDR), emphasizing the urgent need for finding novel and effective drugs against MDR *M. tuberculosis* strains [1].

Abbreviations

4'-PP, 4'-phosphopantetheine; AchE, acetylcholinesterase; DTNB, 5,5'-dithiobis (2-nitrobenzoic) acid; FICI, fractional inhibitory concentration index; HMG-CoA, 3-hydroxy-3-methylglutaryl-CoA; MAFP, methyl arachidonyl fluorophosphonate; MDR, multidrug-resistant; MIC, minimal inhibitory concentration; MS, mass spectrometry; PDIM, phthiocerol dimycocerosates; PGL, phenolic glycolipids; SEC, size-exclusion chromatography; TB, tuberculosis; TE, thioesterase; TesA, thioesterase A; THL, tetrahydrolipstatin; WT, wild-type.

Many pathogenic slow-growing mycobacteria such as *M. tuberculosis*, *M. bovis* and *M. leprae*, harbor an unusual waxy cell envelope [2]. From the inside to the outside, the mycobacterial cell wall consists in peptidoglycan, covalently linked to arabinogalactan further esterified by mycolic acids. Several complex extractible lipids/glycolipids are embedded at the outer surface of the envelope, further enhancing the impermeability [2]. Among these, the related phenolic glycolipids (PGL) and phthiocerol dimycocerosates (PDIM), consisting in either glycosylated phenolphthiocerols or phthiocerols esterified with two polyketide synthase-derived multimethyl-branched mycocerosic acids, have been reported to participate in virulence, drug resistance, and host–pathogen interactions [3–9].

The gene cluster related to PDIM and PGL synthesis is therefore considered as a ‘virulence gene cluster’ in *M. tuberculosis* [10–12]. This cluster encodes various proteins, including the phthiocerol or phenolphthiocerol polyketide synthases (PpsA–E), the mycocerosic acid synthase, fatty acid AMP ligases, the thioesterase A (TesA), and proteins involved in lipid export [12–14]. The PpsA–E processes the elongation of long-chain fatty acids (C20–C22) by adding malonyl-CoA or methylmalonyl-CoA extender units [2]. The release of the phthiocerol and phenolphthiocerol chains from PpsE probably requires TesA thioesterase (TE) activity as indicated by the *in vitro* interaction of TesA with the C-terminal region of PpsE [13] and the absence of PDIM and PGL lipids in *tesA* deletion mutant of *Mycobacterium marinum* [4,9]. The requirement of TesA in PDIM biosynthesis was further confirmed in *M. tuberculosis* as mycobacterial *tesA* disruption mutants were reported to be devoid of PDIM [14,15]. Mycobacterial TesA may be therefore considered as an interesting target to develop new antituberculous drugs. *M. tuberculosis* TesA belongs to the TE-II family [16] and its X-ray structure that fits the structure fold of the α/β -hydrolase superfamily [17] has revealed the presence of a lid subdomain covering its active site [4,17]. Although, first characterization of recombinant TesA enzymatic activities has also been previously reported [17], the exact mechanism behind TesA requirement for PDIM biosynthesis was never demonstrated. Indeed, the expected reaction of the membrane bound [18] TesA hydrolyzing the thioester bond between a phthiocerol (C33–C41) bound to the 4'-phosphopantetheine (4'-PP) arms of acyl carrier protein (ACP) domains of the PpsE protein – PpsE being also bound to the transmembrane Mmpl7 transporter – was not yet studied due to its complexity [19].

The recent crystal structure analysis of *M. tuberculosis* TesA has confirmed Ser104–His236–Asp208 as the catalytic triad [17].

Herein, we report a detailed characterization of the TE activity of the recombinant *M. tuberculosis* TesA. In the presence of the long-chain TE substrates, we demonstrate that TesA undergoes a substrate dependent dimerization. Furthermore, as found with the CyC analog inhibitor, we showed that the methyl arachidonoyl fluorophosphonate (MAFP) can inhibit TesA activities by forming a covalent bond with the catalytic serine residue. We also observed that MAFP increased *M. bovis* BCG susceptibility to vancomycin, and that such effect is counteracted when TesA was overproduced by the mycobacteria, therefore supporting the essential role of TesA in PDIM biosynthesis and confirming the impact of PDIM on vancomycin susceptibility.

Materials and methods

Chemicals

5, 5'-dithiobis (2-nitrobenzoic) acid (DTNB, Ellman's Reagent), BSA essentially fatty acid free, malathion, hexylphosphonic acid, and 4-nitrophenyl acetate were purchased from Sigma Aldrich (St. Louis, MO, USA). Tetrahydrolipstatin (THL) was purchased from Cayman Chemical (Ann Arbor, MI, USA). MAFP was from Sigma Aldrich. The PageRuler™ Prestained Protein Ladder was from Thermo Fisher Scientific (Waltham, MA, USA). All TE substrates were from Santa Cruz Biotechnology (Santa Cruz, CA, USA). Substrates and inhibitor candidates are depicted in Fig. S1. Fresh stock solutions of MAFP, THL, and hexylphosphonic acid were prepared in DMSO (10 mM). Malathion stock solution (10 mM) was prepared in H₂O. The 4-nitrophenyl acetate stock solution (400 mM) was prepared in acetonitrile.

Cloning, expression, and purification

The DNA coding sequence corresponding to *tesA* was amplified by PCR from *M. tuberculosis* genomic DNA. The primers TesA-Fw 5'-GGA ATC CAT ATG CTG GCC CGT CAC GGA-3' and TesA-Rv 5'-GGA ATC CTC GAG CTA AGC TCG ATC ATG-3' were designed to introduce *NdeI* and a *XhoI* restriction site at the 5' and 3' end of the coding sequence, respectively. The amplified *tesA* coding sequence was cloned into a modified pET-15b vector with a cleavage site for the human rhinovirus 3C protease introduced between *NcoI* and *NdeI* to replace the thrombin cleavage site (Fw: 5'-GAT ATA CCA TGG GTA CCA TGC ATC ATC ATC-3' and Rv: 5'-ATC GAT CAT ATG TGG GCC TTG AAA AAG-3'). Consequently, the cloned sequence allowed for a N-terminal five histidine tag sequence followed by a human rhinovirus 3C protease cleavage site before the sequence of the target gene (*tesA*). The constructed plasmid verified by sequencing was transferred into BL21(DE3) *Escherichia coli* strain for protein production.

Briefly, for protein production, the BL21(DE3) *E. coli* strain were grown at 37 °C in Luria-Bertani medium containing 100 µg·mL⁻¹ ampicillin. When the culture reached an OD₆₀₀ of 0.5, protein expression was induced overnight at 18 °C by addition of 1 mM isopropyl β-D-1-thiogalactopyranoside.

The cells were collected and resuspended in a lysis buffer (20 mM HEPES pH 8.0, 300 mM NaCl, 20 mM MgSO₄, 10 mM imidazole, EDTA-free protease inhibitor cocktail, and DNase 10 µg·mL⁻¹), then lysed by three passages in the EmulsiFlex-C3 (Avestin, Ottawa, Ontario, Canada) at 4 °C. The cell lysate was centrifuged for 30 min at 10 800 *g* at 4 °C (rotor SA-300 – Sorvall RC26 Plus) and the supernatant was collected for purification on Ni-NTA agarose column (Thermo Fisher Scientific) at 4 °C. The protein was eluted in 20 mM HEPES, 300 mM NaCl, pH 8.0 containing 250 mM imidazole and further applied on a PD-10 desalting column (GE Healthcare, Boston, MA, USA) to remove the imidazole. The 5× His-tagged protein was incubated overnight at 4 °C in the presence of the protease 3C (TesA/enzyme mass ratio of 75 : 1) for His-tag removal. The protein was further purified by size-exclusion chromatography (SEC) using Superdex 200 10/300 GL analytical column connected to an ÄKTA purifier system (GE Healthcare). The purity and integrity of the TesA protein, concentrated using a Vivaspın 500 centrifugal concentrator with a 5000 Da cutoff (Sartorius, Goettingen, Germany), were analyzed by SDS/PAGE and mass spectrometry (MS), respectively.

TesA thioesterase activity assay

Thioesterase activity was performed in 96-well plate for spectrophotometric measures at 412 nm in order to detect the reaction of the DTNB with thiol groups, yielding a colored product as previously described [17,20]. Briefly, palmitoyl-CoA, decanoyl-CoA, 3-hydroxy-3-methylglutaryl CoA (HMG-CoA), and malonyl-CoA were used as substrates. The stock solutions (10 mM) of each substrate were freshly prepared in 100 mM sodium phosphate (pH 7.2). The reaction medium contained 100 mM sodium phosphate (pH 7.2), 2.5 mM DTNB, BSA and the enzyme in a final volume of 200 µL. The TE activity was followed by monitoring the absorbance over time at 412 nm using spectrometer (Tecan, Männedorf, Switzerland). A $\epsilon_{412} = 14\ 150\ \text{M}^{-1}\text{cm}^{-1}$ was used to calculate the activity. BSA was added at a BSA/acyl-CoA molar ratio of 1 : 4.5 [21]. The TE activity assay was performed with 5 µM TesA and increasing concentrations of substrates. TE activity is expressed in international units (U), corresponding to 1 µmol of TNB²⁻ released per minute. Specific TE activity (SA) is expressed as mU·mg⁻¹ of pure enzyme. First, we calculated the specific TE activity in 1 mL (unit·mL⁻¹): $((\Delta A_{412\ \text{nm}}/\text{minTest} - \Delta A_{412\ \text{nm}}/\text{minBlank})/\epsilon_{412} \times V_e) \times 0.2\ \text{mL}$ (=volume of reaction) \times df (=dilution factor); V_e being the volume (mL) of used enzyme.

Then we calculated the specific activity in unit per mg enzyme knowing the concentration of mg enzyme per mL. Curve fitting and evaluation of apparent K_m and apparent V_{max} [22] were done using OriginPro 8.0 enzyme kinetics program.

TesA esterase assay

The esterase activity assay was performed according to Nguyen *et al.* [17]. The reactions were performed over a period of 30 min. in a 96-well plate in 100 mM sodium phosphate (pH 7.6) containing 2.5 µM TesA, 2 mM 4-nitrophenyl acetate and in the presence or absence of 0.5% (v/v) Triton X-100. The absorbance was measured at 410 nm (spectrophotometer; Tecan). To evaluate the effect of MAFP on the TesA esterase activity, TesA and MAFP were preincubated 30 min at 37 °C before the esterase assay, as previously described with another inhibitor [17]. The residual activity in absence of inhibitor was considered as 100%.

TesA thioesterase inhibitor screening

The reactions were performed without BSA in the presence of 75 µM palmitoyl-CoA. Method A: Dose–response experiments were performed in 200 µL by mixing all components [TesA (5 µM), DTNB (2.5 mM), palmitoyl-CoA (75 µM), and potential inhibitor] to measure TesA TE activity. The absorbance was continuously read every 30 s at 412 nm for 60 min. Method B: Dose–response experiment was based on the preincubation of TesA (in the presence or absence of 0.5% v/v Triton X-100) and MAFP before measuring the TesA TE activity. TesA (20 µM) was preincubated with MAFP at different molar ratios for 5–20 min. The absorbance of the final mixture (200 µL) after the addition of palmitoyl-CoA and DTNB was read at 412 nm for 60 min. In each experiment, two controls were included. The first control was performed with the same volume of solvent but without inhibitor. The second control was performed replacing TesA solution by the same volume of 50 mM Tris-HCl, pH 7.5, 150 mM NaCl. DMSO final concentration was always less than 1.5% in each experiment.

TesA thermal stability assay

The SYPRO orange dye (Thermo Fisher Scientific) was used to monitor protein unfolding. The thermal shift assay was conducted in 96-well plate using the CFX96™ real-time system (Bio-Rad, Hercules, CA, USA) under different conditions (50–800 mM salt, pH, 5–20 µM MAFP). TesA (5 µM) and diluted (2000 times dilution of the commercial stock) SYPRO orange were present in all reactions in the presence of 150 mM NaCl, 50 mM MES buffer (pH 5.5, 6.5), or Tris-HCl buffer (pH 7.5, 8.5). The samples were heated from 20 to 80 °C with a heating rate of 1 °C·min⁻¹.

The fluorescence intensity was recorded at Ex/Em = 465/510 nm. The data were obtained from the Bio-Rad Precision Melt Analysis software 1.0 and exported as Microsoft Excel spreadsheet. Plots of dF/dT (fluorescence intensity difference, dF , in function of temperature difference, dT) were obtained using the ORIGINPRO 8 software (OriginLab Corporation, Northampton, MA, USA).

Mass spectrometry analysis of TesA-MAFP interaction

Methyl arachidonyl fluorophosphonate was added to TesA (20 μM) at a MAFP/protein molar ratio of 4 : 1 in 100 mM sodium phosphate pH 7.2. The mixture was incubated at 37 °C for 1 h. To remove free MAFP, SEC (Superdex 200 10/300 GL) was performed in 50 mM Tris-HCl, 150 mM NaCl, pH 7.5. PD MiniTrap™ G-25 (GE Healthcare) column was used to change the elution buffer to 10 mM ammonium acetate (pH 6.9). Samples (~ 10 μg protein) were lyophilized and dissolved in 5 μL of 50% acetonitrile/1% formic acid (v/v). The intact mass of the MAFP/TesA complex was analyzed by MS. The samples were loaded into a nanoflow capillary (Thermo Fisher Scientific). ESI mass spectra were acquired on a quadrupole time-of-flight instrument (Q-ToF Ultima – Waters/Micromass) operating in the positive ion mode, equipped with a Z-spray nano-electrospray source. The spectra were recorded in the V mode and represent the combination of 1 s scans. The molecular mass of the protein was determined after processing of the m/z spectra with the software MaxEnt 1 (Waters, Milford, MA, USA).

After the SEC, 10 μg MAFP-TesA complex and TesA was kept for enzymatic digestion. The proteins were incubated at 37 °C for 16 h in the presence of sequencing grade trypsin/Lys-C (Promega, Madison, WI, USA) at an enzyme/protein mass ratio of 1 : 25 in 50 mM Tris-HCl, 150 mM NaCl, pH 7.5. Peptides were dissolved in solvent A [0.1% TFA in 2% ACN (v/v)], directly loaded onto reversed-phase precolumn (Acclaim PepMap 100; Thermo Scientific) and eluted in backflush mode. Peptide separation was performed using a reversed-phase analytical column (Acclaim PepMap RSLC, 0.075 \times 250 mm; Thermo Scientific) with a linear gradient of 4%–27.5% solvent B [0.1% FA in 98% ACN (v/v)] for 100 min, 27.5–40% solvent B for 10 min, 40–95% solvent B for 1 min, and holding at 95% for the last 10 min at a constant flow rate of 300 nL·min⁻¹ on an EASY-nLC 1000 UPLC system. The resulting peptides were analyzed by Orbitrap Fusion Lumos tribrid mass spectrometer (ThermoFisher Scientific). The peptides were subjected to NSI source followed by tandem mass spectrometry (MS/MS) in Fusion Lumos coupled online to the UPLC. Intact peptides were detected in the Orbitrap at a resolution of 120 000. Peptides were selected for MS/MS using HCD setting as 30; ion fragments were detected in the Orbitrap at a resolution of 30 000. A data-

dependent procedure alternating between one MS scan followed by 20 MS/MS scans was applied for the top 20 precursor ions above a threshold ion count of 5.0×10^3 in the MS survey scan with 20.0 s dynamic exclusion. The electrospray voltage applied was 2.1 kV. MS1 spectra were obtained with an AGC target of 4E5 ions and a maximum injection time of 50 ms, and MS [2] spectra were acquired with an AGC target of 5E4 ions and a maximum injection time of 100 ms. For MS scans, the m/z scan range was 350–1500. The resulting MS/MS data were processed using Sequest HT search engine within Proteome Discoverer 2.2 against a homemade protein database containing the recombinant TesA sequence. Trypsin/Lys-C was used as cleavage enzyme allowing up to two missed cleavages, five modifications per peptide, and up to seven charges. Mass error was set to 10 p.p.m. for precursor ions and 0.2 Da for fragment ions. False discovery rate was assessed using a fixed value PSM validator, and thresholds for protein, peptide, and modification site were specified at 1%. Site of covalent modification with MAFP was manually validated.

TesA oligomeric state determination

TesA was analyzed by SEC using a Superdex 200 GL 10/300 column. Fifty microlitre of purified TesA (5 μM in 50 mM phosphate buffer pH 6.8) was injected on the column pre-equilibrated in the same buffer. For TesA analysis in the presence of thioester substrate, 15 mL of a palmitoyl-CoA solution (100 μM in 50 mM phosphate buffer pH 6.8) were injected on the column prior to TesA injection. Aliquots of 0.5 mL were collected at the column output and analyzed for protein content using the Bradford assay. Data are represented as smoothed curves. Calculated molecular weights were obtained based on the elution profile of gel filtration standards (mixture of thyroglobulin, gamma-globulin, ovalbumin, myoglobin, and vitamin B12 from Bio-Rad).

TesA overexpression in *M. bovis* BCG

Mycobacterium bovis BCG electrocompetent cells were prepared according to previous reports [23,24]. For electroporation, we used the MicroPulser™ Electroporator (Bio-Rad) system. Briefly, 150 μL competent *M. bovis* BCG cells was mixed with 1 μg of pVV16-tesA plasmid DNA [23] and transferred to a 2 mm gap cuvette (VWR). After a signal pulse of 3.0 kV, 5 mL Dubos medium (Becton, Dickinson and Company) supplemented with 10% (v/v) albumin (Sigma Aldrich) was immediately added to the suspension, followed by incubation at 37 °C for 12 h with shaking. Bacteria were then plated on the 7H11 mycobacteria agar supplemented with 10% OADC containing kanamycin (50 $\mu\text{g}\cdot\text{mL}^{-1}$) and hygromycin (100 $\mu\text{g}\cdot\text{mL}^{-1}$). After 2 week incubation at 37 °C, colonies, corresponding to *M. bovis* BCG-overTesA, were harvested for further experiments.

Drug susceptibility assay

Mycobacterium bovis BCG strains were grown in 25 cm² flasks at 37 °C without shaking in Dubos medium (Becton, Dickinson, Franklin Lakes, NJ, USA) supplemented with 10% (v/v) albumin (Sigma Aldrich) to an OD₆₀₀ of 0.3–0.9. The macrodilution method was performed in 12 mL screw tubes in 7H9 medium (Becton, Dickinson and Company) containing 0.05% glycerol and 10% albumin–dextrose complex. Five hundred microlitre inoculum diluted in the supplemented 7H9 medium to reach an optical density at 600 nm (OD₆₀₀) of 0.01 was added to 500 µL serial drug dilutions in the same 7H9 medium. Tubes were placed at 37 °C without shaking. Growth or absence of growth was recorded on the day that the growth of the 100-fold diluted drug-free inoculum control became visible in order to assess the minimal inhibitory concentration of the drugs (MIC, being the lowest drug concentration inhibiting more than 99% of *M. bovis* BCG strain bacterial growth) [25]. This experiment was performed three times to check the reproducibility of the MIC determination. The fractional inhibitory concentration index (FICI) was calculated according to the checkerboard method, as follows: $FICI = FIC_a + FIC_b = MIC_{ab}/MIC_a + MIC_{ba}/MIC_b$. The MIC of the MAFP and vancomycin alone (MIC_a and MIC_b, respectively), the MIC of the MAFP in combination with a fixed vancomycin concentration (MIC_{ab}), and inversely the MIC of the vancomycin in combination with a fixed MAFP concentration (MIC_{ba}) were obtained. The fixed concentrations were 4- and 20-fold lower than the MIC_a or MIC_b, respectively. In agreement with the checkerboard method, synergy is reached when the FICI is < 0.5 [25].

Docking protocols

The X-ray structure of TesA determined in complex with hexadecyl dihydrogen phosphate CyC₁₇ (PDB: 6FVJ) was used as the target structure to endeavor the docking studies [17]. Chain A was selected for the docking calculations into the monomeric structure of TesA and chains A and F were selected for the dimeric structure. The X-ray water and other ligand molecules were removed from the active site. The TesA crystal structure was prepared with the Protein Preparation Wizard workflow implemented in the Schrödinger package [26]. The initial 3D structures of the ligands were generated using the Ligprep module (Schrödinger, LLC, New York, NY, USA, 2018). In the present work, the binding region in the monomer was defined by a box centered on the phosphorus position of the 4-carbon long truncated crystal CyC₁₇ with a box length of 38 Å. Docking was performed using the Glide SP docking protocol and scoring function which approximates a systematic search of positions, orientations, and conformations of the ligand in the receptor binding site using a series of hierarchical filters [27]. The default settings of Glide were used.

Results

Recombinant TesA expression and purification

The recombinant protein was overexpressed in a BL21 (DE3) *E. coli* strain and purified by immobilized metal affinity chromatography. After cleavage of the His-tag, TesA was further purified by size-exclusion chromatography (SEC, Fig. S2B-a). The purity of recombinant TesA was determined by 12% SDS/PAGE and a single band with an apparent molecular weight of ~ 27 kDa was observed after Coomassie Brilliant Blue staining (Fig. S2B-b). After His-tag cleavage, three additional N-terminal residues (Gly-Pro-His) (Fig. S2A) remain fused to TesA leading to a theoretical molecular mass of 29 443 Da. The experimental molecular mass of 29 443 Da determined by MS totally agrees with this theoretical value (Fig. S2B-c).

The recombinant TesA stability properties were investigated by thermal shift assay. We examined the impact of NaCl, pH, and MAFP on TesA thermal stability (Fig. S2C) and observed that increasing concentrations of NaCl and MAFP had a stabilizing effect on the protein. The protein was also more stable between pH 6.5 and 8.5.

Thioesterase activity of recombinant TesA

We first monitored TesA TE activity using palmitoyl-CoA as thioester substrate at different temperatures (4, 22, and 37 °C), and observed that the optimal temperature was 37 °C (data not shown). The addition of fatty acid-free BSA, that could reduce inhibition of TE activity at high substrate concentrations, improved the catalytic activity of TesA, as previously observed for various thioesterases [21]. Control experiments were performed in the absence of different component to exclude nonspecific influence on reaction (data not shown).

We tested TesA TE activity toward four different CoA-derived substrates (Fig. S1A). Our results using palmitoyl-CoA, HMG-CoA, and malonyl-CoA fitted to the apparent Michaelis–Menten model (Fig. 1A,C, D). The enzyme displayed a higher specific TE activity (SA) for the long-alkyl chain and hydrophobic substrates, palmitoyl-CoA (C16-SA = 34.8 mU·mg⁻¹), and decanoyl-CoA (C10-SA = 46.2 mU·mg⁻¹). Malonyl-CoA and HMG-CoA were not good substrates for the TesA TE, as demonstrated by their specific activity of 3.5 and 5.1 mU·mg⁻¹, respectively. Moreover, the apparent V_{max} ($^{app}V_{max}$) ($1.71 \pm 0.39 \times 10^{-8}$ M·s⁻¹) of the reaction was about one-order of magnitude faster (P value < 0.05) with a long-chain substrate

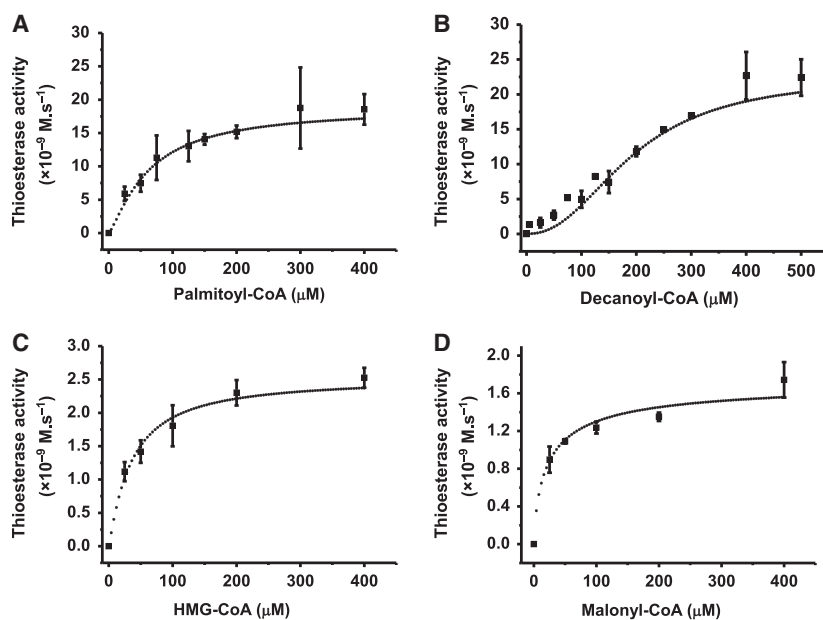


Fig. 1. Acyl-CoA thioesterase activity of purified recombinant TesA in the presence of different substrates: (A) palmitoyl-CoA, (B) decanoyl-CoA, (C) HMG-CoA, and (D) malonyl-CoA. The thioesterase activity assay was performed with 5 μM TesA, 2.5 mM DTNB, BSA, and an increasing concentration of substrate at 37 °C. BSA was added at a BSA/acyl-CoA molar ratio of 1 : 4.5. The data correspond to means and standard deviations from at least three independent experiments.

Table 1. Apparent (app) kinetic parameters of recombinant TesA with a series of different acyl-CoA as substrates.

Substrate	$^{app}V_{\text{max}}$ ($\text{M}\cdot\text{s}^{-1}$)		$^{app}K_{\text{m}}$ (μM)		$^{app}k_{\text{cat}}$ (s^{-1})	
	Value	SD	Value	SD	Value	SD
Decanoyl-CoA	NA	NA	–	–	NA	NA
HMG-CoA	2.53×10^{-9} *	1.49×10^{-10}	42.42 ± 7.7	7.697	5.05×10^{-4}	2.99×10^{-5}
Palmitoyl-CoA	1.71×10^{-8}	3.89×10^{-9}	57.44	9.50	3.42×10^{-3}	7.78×10^{-4}
Malonyl-CoA	1.74×10^{-9} *	1.88×10^{-10}	27.64	11.33	3.49×10^{-4}	3.76×10^{-5}

The $^{app}V_{\text{max}}$ values with a symbol (*) are significantly different ($P < 0.05$) compared the value palmitoyl-CoA. NA, not applicable.

(C16) compared to HMG-CoA and malonyl-CoA (Table 1). The affinity to substrate ($^{app}K_{\text{m}}$) of HMG-CoA and malonyl-CoA were evaluated to be $42.4 \pm 7.7 \mu\text{M}$ and $27.6 \pm 11.3 \mu\text{M}$, respectively. The best turnover number ($^{app}k_{\text{cat}}$) was for palmitoyl-CoA (3.42 ± 0.78) $\times 10^{-3}\cdot\text{s}^{-1}$. A sigmoidal curve was observed with decanoyl-CoA, suggesting a potential conformational change in the enzyme with this substrate [28]. An oligomeric state of TesA endowed with a homotropic activation mechanism may explain this observation [29].

Since the TesA natural substrate featured a β -methyl group in the phthiocerol derived thioesters (C31–C33) bound to the mycobacterial PpsE protein [13], we also evaluated TesA TE activity using the methylmalonyl-CoA as substrate. TesA exhibited similar activity (P value > 0.05) on methylmalonyl-CoA and malonyl-CoA ($SA = 3.6 \text{ mU}\cdot\text{mg}^{-1}$ and $SA = 3.5 \text{ mU}\cdot\text{mg}^{-1}$, respectively) (data not shown).

The addition of 0.5% Triton X-100, recently reported to activate TesA esterase activity [17],

reduced TesA TE activity (P value < 0.05) using either palmitoyl-CoA (Fig. S3) or malonyl-CoA (data not shown) as substrate.

Oligomeric state of TesA

Size-exclusion chromatography was performed to evaluate the TesA oligomeric states (Fig. 2). Alone, the enzyme behaves as a monomer. However, the addition of palmitoyl-CoA into the SEC column with low enzyme concentration, in order to reduce substrate consumption during the assay, led to the protein elution at a lower retention volume with a native molecular weight close to 68 kDa, indicative of a dimeric state.

Influence of potential inhibitors on TesA activities

We first investigated the ability of four inhibitor candidates to inhibit TesA TE activity. Hexylphosphonic

acid and malathion have been selected because of their reactive organophosphate group. Malathion is known to irreversibly inhibit the acetylcholinesterase (AChE) after binding to the serine residue of AChE catalytic site [31]. The THL (Orlistat) was chosen because it was previously shown to interact with various α/β -hydrolases, including TesA [17,30], and the MAFP was tested because it is a well-established irreversible inhibitor for most serine enzymes, including some phospholipases [32]. When the inhibition assay was

performed by using the method A – that is competitive inhibition mixing altogether TesA (5 μM), the inhibitor, the DTNB and the palmitoyl-CoA into the 96-well plate – hexylphosphonic acid and malathion had no influence on TesA TE activity. In contrast, MAFP and, to a lesser extent, THL inhibited TesA TE activity (Fig. 3) in a concentration-dependent manner. With MAFP, a maximal 52% inhibition was observed in all tested experimental conditions, for example the competitive assay (Method A) or by preincubating TesA

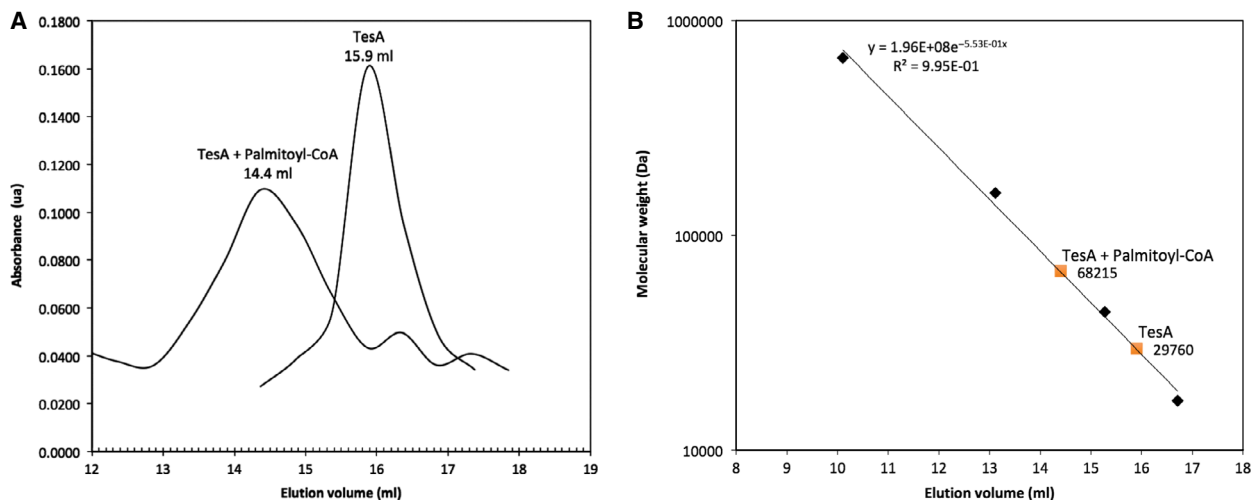


Fig. 2. Gel filtration chromatography of TesA and TesA/palmitoyl-CoA complex. (A) TesA and TesA/palmitoyl-CoA complex, (B) Elution of standard molecular mass marker proteins. Black diamonds: gel filtration standard; orange squares: TesA.

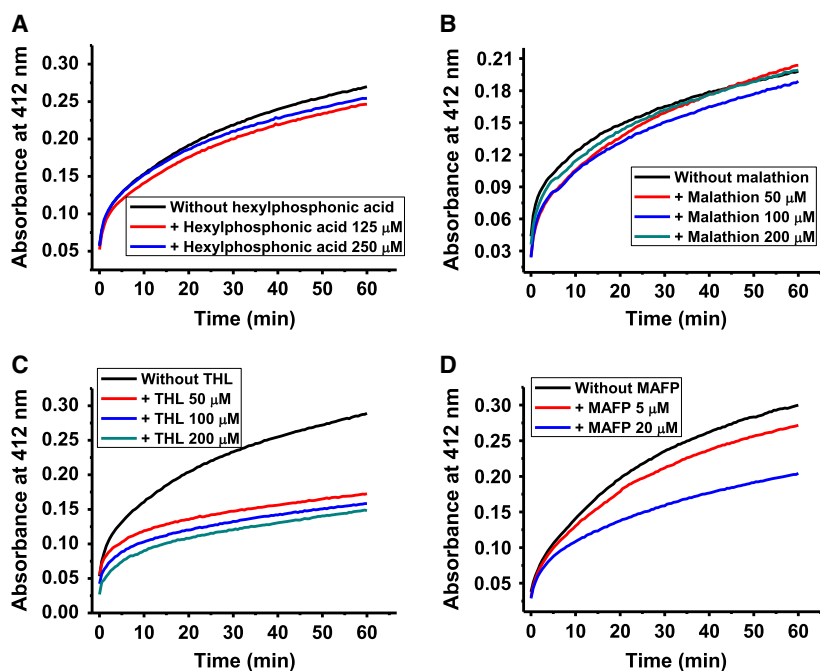


Fig. 3. Effect of different inhibitors on TesA thioesterase activity. A–D. Method A - The reaction medium (200 μL) contained 5 μM TesA, 75 μM palmitoyl-CoA, 2.5 mM DTNB, with or without inhibitor. (A) hexylphosphonic acid, (B) malathion, (C) THL, and (D) MAFP, all components were added together in the reaction medium. Each plot is representative of three independent experiments.

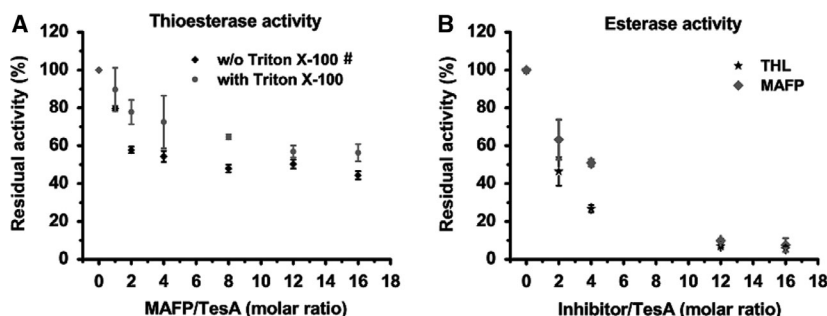


Fig. 4. Residual activity of TesA. (A) Inhibition of thioesterase activity assay by MAFP. TesA was preincubated with various concentrations of MAFP for 5 min. The reaction contained enzyme/inhibitor mixture, 10 mM DTNB, 75 μ M palmitoyl-CoA, with or without 0.5% (v/v) Triton X-100 in 100 mM sodium phosphonate buffer (pH 7.6). The data obtained in absence of Triton X-100 are significantly different ($P < 0.05$) than those in the presence of Triton X-100. (B) Inhibition of esterase activity assay by MAFP or THL. TesA (2.5 μ M) was preincubation with various concentration of MAFP or THL for 30 min. The reaction contained enzyme/inhibitor mixture, 2 mM 4-nitrophenyl acetate, 0.5% (v/v) Triton X-100 in 100 mM sodium phosphonate buffer (pH 7.6). The activity without inhibitor was considered as 100%. The data correspond to means and standard deviations from at least three independent experiments.

(Method B) with MAFP for 5 or 20 min before starting the reaction with palmitoyl-CoA. In order to potentially increase the access of MAFP to the TesA catalytic site, we tested the impact of Triton X-100 in the reaction. The presence of this surfactant during preincubation of TesA with MAFP unexpectedly reduced MAFP inhibitory activity ($P < 0.05$) in the presence of palmitoyl-CoA (Fig. 4A). It is worth noting that although at the used concentration, palmitoyl-CoA forms micelles [33] in solution; addition of Triton X-100 has however been reported to have a negative impact on such micelles formation [34]. Furthermore, this nonionic detergent could also interfere with the hydrophobic interactions between the MAFP and TesA (see our docking analysis hereunder). This might explain the tendency of Triton X-100 to decrease the MAFP induced inhibition (Fig. 4A).

In parallel, we investigated the ability of MAFP and THL to inhibit TesA esterase activity on the small 4-nitrophenyl acetate substrate. Preincubation with both MAFP and THL inhibited TesA esterase activity in a concentration-dependent manner. The MAFP inhibitor appeared to fully inactivate TesA esterase activity while it only reduced by approximately 50% TesA TE activity using palmitoyl-CoA as substrate (Fig. 4B).

Mass spectrometry analysis of TesA-MAFP interaction

TesA incubated in the presence of MAFP at a protein/inhibitor molar ratio of 1 : 4 was analyzed by MS. As shown in Fig. 5, two main peaks at molecular masses of 28 543 and 28 894 Da, and two minor ones at

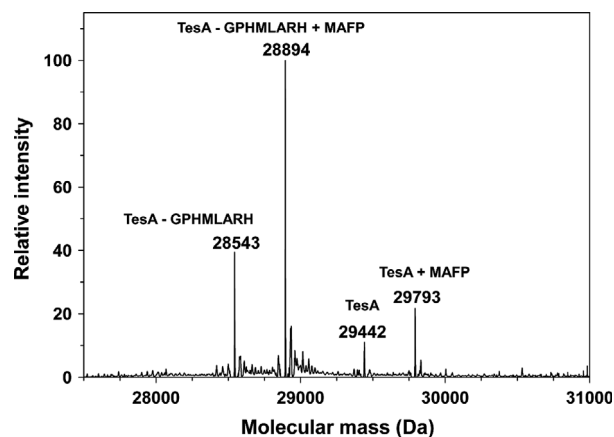


Fig. 5. TesA-MAFP complex analysis by MS. Mass spectrum showing the presence of TesA alone or modified by MAFP. 'TesA - GPHMLARH' corresponds to the N-terminal degradation of the protein resulting in the loss of the first eight residues.

29 442 and 29 793 Da were observed. The two minor peaks correspond to the intact TesA (theoretical molecular mass 29 443.1 Da), and to the TesA/MAFP covalent adduct, respectively. The MS analysis shows that a fraction of TesA is not bound by the MAFP (Fig. 4A). The two main peaks also correspond to TesA (28 543 Da) and to the MAFP-modified TesA (28 894) but in both cases, the N terminus of TesA was shortened by the loss of the GPHMLARH residues (Fig. S2A), as calculated from the protein sequence (theoretical molecular masses: 28 543.1 and 28 893.6 Da, respectively). This N-terminal degradation could be due to TesA proteolysis by a protease present in trace amounts in the TesA preparation that could have digested TesA during the different steps of

the experiment. The mass shifts observed in the presence of MAFP are consistent with the covalent binding of the inhibitor on TesA with the loss of one hydrogen and one fluorine atom (theoretical Δ mass = 350.5 Da) [32]. After trypsin/Lys-C digestion of the TesA/MAFP complex, the resulting peptides were microsequenced by MS/MS. As expected, the Ser104 was identified as the residue covalently modified by MAFP (Fig. S4).

Docking calculations

To rationalize the data showing that palmitoyl-CoA is a better substrate than malonyl-CoA and that MAFP only inhibits 50% of TesA TE activity in presence of palmitoyl-CoA, we docked this substrate and inhibitor in the 3D structure of TesA [17].

First, to validate our procedure, the noncovalent docking of the propyl phosphate was performed and compared with the crystal position of the 4-carbon

long truncated hexadecyl dihydrogen phosphate. The phosphate group occupied the same position in the docked poses and in the experimental crystal structure therefore validating our docking procedure to evaluate other compounds (Fig. S5).

The docked poses of palmitoyl-CoA in the binding site of the monomeric TesA show one type of binding mode which features the thioester group close to the active site Ser104 and His236 (Fig. 6A,B). Docking calculations of palmitoyl-CoA were also performed in the TesA dimer with poses similar to those found for the monomer (Fig. 6C), except for one top score pose, showing one palmitoyl phosphate matching with the crystal phosphate. Remarkably, in the binding modes, the alkyl chain of palmitoyl-CoA positions itself at the surface of the monomer, facing the other monomer in the dimer (Fig. 6B,D). This layout could contribute in promoting the dimerization of the protein, as we observed by SEC.

In contrast to palmitoyl-CoA, the docked poses of malonyl-CoA in the monomer present a variety of

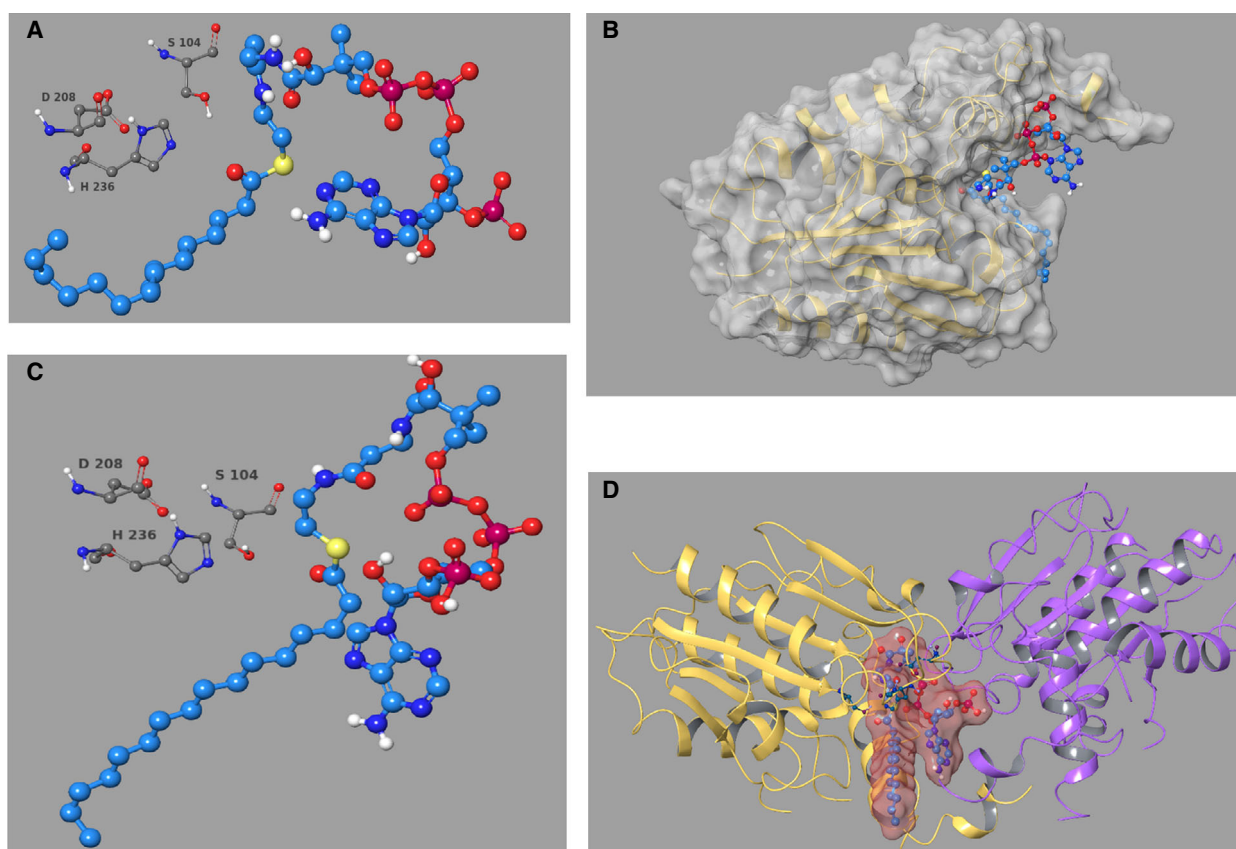


Fig. 6. Molecular docking in TesA monomer and dimer. (A and C): Close view of the binding pose of palmitoyl-CoA featuring its thioester carbonyl group in the catalytic site of TesA monomer (A) and dimer (C); B: Molecular surface of TesA monomer bound to the palmitoyl-CoA binding pose as shown in A; D: Molecular surface of palmitoyl-CoA bound in one catalytic site of TesA dimer as shown in C. Palmitoyl-CoA is represented as ball-and-sticks and the catalytic residues (Ser104, Asp208 and His236) as sticks. In B and D, TesA is depicted as yellow and purple cartoon.

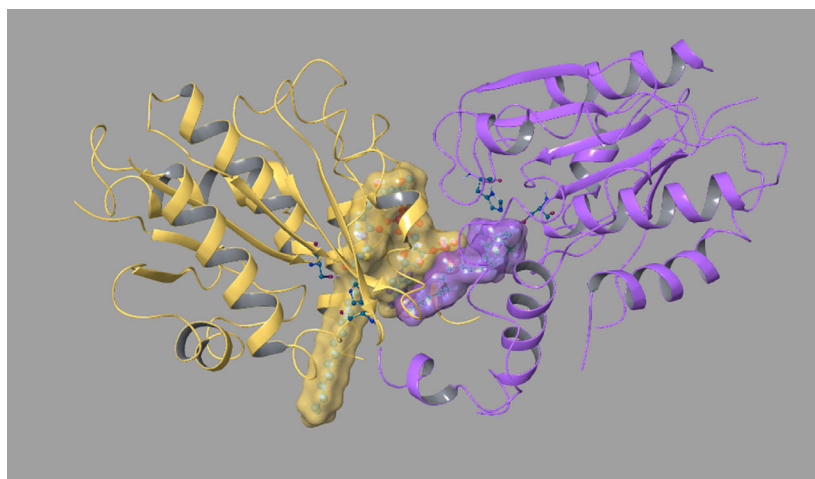


Fig. 7. Binding mode of MAFP bound in one of the two catalytic sites of the TesA dimer bound to palmitoyl-CoA in the other site (pose shown on Fig. 6C,D). Molecular surfaces of MAFP and palmitoyl-CoA are colored in yellow and purple respectively. Each TesA monomer is depicted as a yellow and purple cartoon.

binding modes in which either the carboxylate or one of the phosphate groups or the thioester group fit a position corresponding to the crystal phosphate ligand group. These data might explain why the malonyl-CoA is a poorer substrate than the palmitoyl-CoA.

For MAFP, the best score docked poses show a large variability in binding modes, including one position with the fluorophosphonate group matching the crystal ligand phosphate.

Finally, MAFP and palmitoyl-CoA were also docked into one of the two binding sites of the dimer featuring one palmitoyl-CoA molecule previously bound by docking into the other active site (Fig. 6C). Most of the MAFP poses occupy the second binding site with the fluorophosphonate matching the crystal ligand phosphate (Figs 7 and S6). As for palmitoyl-CoA, no pose featuring the thioester group in the catalytic pocket was generated. These findings provide a possible explanation for the 50% TE activity inhibition by MAFP in presence of palmitoyl-CoA if one assumes that palmitoyl-CoA features a better affinity than MAFP for the first binding site which is suggested by the docking scores (-6.6 versus -3.9 kcal·mol⁻¹).

MAFP increases vancomycin susceptibility

As PDIM deficient *M. bovis* BCG and *M. tuberculosis* mutants are specifically more susceptible to vancomycin [8,25], by a 100-fold factor, we assessed the effect of MAFP on *M. bovis* BCG vancomycin susceptibility. MAFP increased by more than 10-fold the susceptibility of *M. bovis* BCG to vancomycin (Table 2). To investigate whether this growth inhibition resulted from a synergy between MAFP and vancomycin, we used the Checkerboard method to calculate the FICI. The MIC of MAFP dropped from ≥ 10 to 1 $\mu\text{g}\cdot\text{mL}^{-1}$ in the presence of vancomycin (25 $\mu\text{g}\cdot\text{mL}^{-1}$), and the MIC of vancomycin dropped from ≥ 500 to 25 $\mu\text{g}\cdot\text{mL}^{-1}$ in the presence of MAFP (1 $\mu\text{g}\cdot\text{mL}^{-1}$), showing that this combination can inhibit *M. bovis* BCG growth in synergy (FICI < 0.15) This synergy would suggest that MAFP inhibited the PDIM biosynthesis [8]. Since TesA could not be the only target, we also considered the possibility that this MAFP effect could be due to its interference with other proteins. To solve this issue, we overexpressed TesA in *M. bovis* BCG. Importantly, overexpression of TesA in mycobacteria abrogated the observed synergy, strongly suggesting that TesA inhibition by MAFP was

Table 2. Vancomycin susceptibility obtained in macrodilution series and analyzed by the checkerboard method for *M. bovis* BCG strains, wild-type (WT), or overexpression TesA (overTesA).

Strain	MIC ($\mu\text{g}\cdot\text{mL}^{-1}$)/FIC ($\mu\text{g}\cdot\text{mL}^{-1}$)/FICI			
	wtWT <i>M. bovis</i> BCG		<i>M. bovis</i> BCG-overTesA	
	Vancomycin	MAFP	Vancomycin	MAFP
Alone	500/–/–	> 10/–/–	250/–/–	> 10/–/–
+ 1 $\mu\text{g}\cdot\text{mL}^{-1}$ MAFP	25/0.05/< 0.15	–/–/–	> 100/> 0.4/> 0.9	–/–/–
+ 25 $\mu\text{g}\cdot\text{mL}^{-1}$	–/–/–	1/< 0.1/< 0.15	–/–/–	> 5/> 0.5/> 0.9

responsible for this synergistic growth inhibitory effect with vancomycin (Table 2).

Discussion

Tuberculosis, caused by *M. tuberculosis*, is the ninth leading cause of death worldwide and the leading cause of death from a single infectious agent [1]. The increase of MDR *M. tuberculosis* strain is alarming, emphasizing the urgent need to find new antitubercular drugs. The mycobacterial TesA protein was reported to be required for PDIM biosynthesis, a lipid from the outermost membrane of the mycobacterial cell wall, necessary, among others, for mature biofilm formation and drug resistance [4,6]. TesA is consequently considered as a potential target in anti-TB drug discovery perspective. We therefore expressed and purified the recombinant *M. tuberculosis* TesA to identify and analyze potential TesA inhibitors. We used acyl-CoA derivatives as substrates as those are mimicking the TesA natural substrate, a fatty acyl, elongated phthiocerol moiety joined by a thioester linkage to the phosphopantetheinyl arm of the ACP domain of the PpsE during PDIM biosynthesis.

Unexpectedly, although the addition of detergent (Triton X-100) increased TesA esterase activity, the TesA TE activity was inhibited in the presence of detergent. This was unexpected, as detergents have been reported to increase TesA esterase activity by promoting and stabilizing a lid opening process [17]. The difference of detergent effects on the TesA esterase and TE activity could be due to the different TesA/substrate interfaces, especially if we consider the water insoluble *p*NP ester substrates used for the esterase activity [17] and the water-soluble long-chain fatty acyl-CoA thioester substrates used in this study. Our hypothesis is that the hydrophobicity of the palmitoyl-CoA acyl chain or its hydrolyzed product following TesA activity could favor TesA dimerization (Fig. 6) and consequently the TE activity. Conversely, in the presence of detergents, this oligomerization could be destabilized. Indeed, our docking model suggests that the long-acyl chain of the palmitoyl-CoA could lie on the external side of TesA (Fig. 6), just at the interface of the crystallized dimer [17], an action that does not occur with the small *p*NP ester substrates used in the esterase assay. Interestingly, it has been previously described that palmitoyl-CoA acts in fact just like a detergent, by forming micelles when its concentration is above its critical micelle concentration which is definitively the case here [34]. Changes in the palmitoyl-CoA micelle solutions composition, that is by the addition of

Triton X-100, have been previously described to inhibit hydrolase activity; while the addition of serum albumin was reported not only to prevent palmitoyl-CoA micelle formation but also to activate the enzyme by interacting with its hydrophobic regions [34,35]. The specific TE activity on palmitoyl-CoA of our recombinant protein ($SA = 34.8 \text{ mU}\cdot\text{mg}^{-1}$) is relatively high in comparison to the previously reported TE activity ($6.82 \text{ mU}\cdot\text{mg}^{-1}$) [17]. The BSA added, here, in our TE assay might have promoted the fatty acid release in the catalytic site. In contrast, the addition of Triton X-100 could have increased the size of the palmitoyl-CoA micelle reducing its accessibility to the catalytic site in the dimeric form, by steric congestion.

Compared to the type III recombinant mycobacterial FcoT TE activity [36], the recombinant TesA TE activity showed a similar binding affinity ($^{3\text{H}}K_m$ value) for palmitoyl-CoA but a 10-fold reduced turnover number ($^{3\text{H}}K_m$ value). The use of a surrogate substrate instead of the expected natural phthiocerol (C33–C41), and the fact that this *in vitro* assay did not mimic TesA *in vivo* steric environment – with a substrate bound to the 4'-PP arms of ACP domains of a huge PKS protein, which is itself also bound to a transmembrane transporter – may explain such difference.

The sigmoidal TE reaction curve observed in the presence of decanoyl-CoA further suggests that TesA could act in an oligomeric state. This is not only in agreement with its X-ray dimeric structure obtained in the presence of covalently bound CyC₁₇ inhibitor [17] but also with our SEC analysis demonstrating the dimeric state of TesA in the presence of palmitoyl-CoA. These results indicated that TesA undergoes a substrate-induced dimerization. It is difficult to know if TesA could dimerize in the bacteria when interacting with its substrate, a C-33 phthiocerol thioester precursor covalently attached to the phosphopantetheinyl arm of PpsE. However, considering the hydrophobic chain of its native substrate and the hydrophobic cavity of the ACP domain, it is possible that such a TesA dimerization could take place.

Some molecules have been reported either to bind TesA, like THL, or to have chemical groups, like phosphonate, with known inhibitory activity for possible interference with TesA catalytic activity [17,30]. The phosphate analog (CyC₁₇) was reported to inhibit TesA esterase activity by covalently binding to the catalytic serine residue [17].

Here, we investigated the impact of four molecules on TesA TE activity. The hexylphosphonic acid and malathion did not affect the TesA TE activity (Fig. 3A,B). As expected, we observed that THL is a

potent inhibitor of TesA TE activity (Fig. 3C), further confirming that THL might be an interesting anti-TB drug candidate [17,37]. Indeed, THL was shown to reduce mycobacteria cell wall lipid biosynthesis, targeting various serine enzymes involved among others in sulpholipids, mycolic acids, or PDIM biosynthesis [25,37–39]. In addition, the effect of THL on the mycobacterial cell wall integrity allowed to improve susceptibility to other drugs, as observed with vancomycin [25]. THL is mainly known as a pancreatic lipase inhibitor, inhibiting the type-I fatty acid synthase on its C-terminal thioesterase domain (TE). This domain hydrolyzes the thioester bond between the palmitate and the 4'-PP moieties of an ACP [40–42]. This TE domain shares the canonical catalytic triad (Ser-His-Asp) with other serine hydrolases [40], including TesA [17]. Analysis of the crystal structure of the TE domain–THL complex in human fatty acid synthase shows that the palmitate-like inhibitor THL binds to the hydrophobic pocket of TE domain [43]. THL is present in two states in the TE active site: either covalently bound to the active-site serine or as a hydrolyzed product. Its hexyl tail in these two different states adopts different conformations, suggesting that the hexyl tail conformation may play a critical role in hydrolysis [41]. It was also reported that THL displayed inhibition on TesA using activity-based profiling [30].

MAFP irreversibly binds and inhibits its targets through phosphorylating active-site serine residues [44]. In MAFP, the C20 alkyl chain on the fluorophosphonate might more easily target TesA catalytic site than the less lipophilic organophosphorus malathion, giving a possible explanation to their different TesA inhibition abilities, despite common ability to attack a nucleophilic serine catalytic residue. Furthermore, MAFP has been reported to be a broad-spectrum Ser active site inhibitor compared to malathion [45–47]. Indeed, the serine-reactive fluorophosphonate (FP) of MAFP inhibited more *M. tuberculosis* esterases than the E-600, THL, and PMSF inhibitors [48]. To better characterize this inhibitor, we preincubated MAFP and TesA at different molar ratios, before measuring the reaction rate with palmitoyl-CoA (Fig. 4A). As expected for a covalent inhibition, a dose-dependent decrease in activity was observed but, surprisingly, the inhibition did not proceed to full inactivation of the enzyme. Around 50% residual activity was constantly observed, even using high molar excess of MAFP (16 : 1). Higher inhibitor concentration could not be used due to low MAFP solubility. The addition of Triton X-100 (Fig. 4A) in the TE assay did not improve the inhibition level. Longer reaction times (up to 1 h)

with a higher MAFP/TesA molar ratio, using a competitive approach, putting all reagents together, or by preincubating the enzyme with the MAFP, also failed to induce more than 45% inhibition. However, MAFP alone could completely inhibit TesA esterase activity using *p*-nitrophenyl acetate as substrate (100% inhibition). This differential effect is thus dependent on the substrate. Possible explanations could be that the position of the palmitoyl hydrolyzed substrate still interacting with TesA could inhibit MAFP/TesA interaction (Figs 7 and S7). Indeed, both molecules could interact with dimer interaction surface. However, this explanation would be satisfactory if the 50% inhibition by MAFP on TesA TE activity was only observed in a competitive experiment, which is not the case. Therefore, there must be another explanation. We believe that during the esterase assay, when using *p*NP-acetate as substrate, TesA stays as a monomer and *p*NP-acetate does not induce dimerization. Indeed, according to our docking studies, long-acyl chain could induce TesA dimerization *via* a hydrophobic interaction which could not take place with the *p*NP-acetate. When MAFP binds TesA, it could induce protein dimerization through its hydrophobic acyl chain, as previously reported in the case of the phosphonate inhibitor CyC₁₇ [17]. Consequently, the second catalytic site in the dimeric form could not be easily reached by the MAFP. Indeed, we observed in MS analysis that a fraction of TesA is not bound by the MAFP. The MAFP-induced dimerization could in turn inhibit the access of *p*NP-acetate to the second catalytic site even in the presence of Triton X-100, as the affinity of the long-acylated MAFP chain could prevent further *p*NP-acetate/TesA interaction or acetate release from TesA catalytic site by hydrolysis [49]. In the TE assay, the presence of palmitoyl-CoA micelles may favor or only allow access to this substrate inside the second MAFP induced, TesA dimeric active-site entrance; thus resulting in 50% TE residual activity. Interestingly, we observed that MAFP can slightly stabilize the TesA protein in thermal shift assay.

Therefore, the enzymatic outcomes using different substrates, the dimerization induced by substrate (palmitoyl-CoA), the 50% TE activity inhibition by MAFP, the potential lid structure obtained from X-ray crystal analysis [17], and our docking analyses are all together suggesting that conformation changes induced by substrate/inhibitor are interfering in TesA function (Fig. S7). Indeed, our TesA-ligands models (Figs 6 and 7) demonstrated that the TesA dimerization induced by the palmitoyl-CoA also could affect the MAFP binding.

Considering that MAFP is targeting more *M. bovis* BCG enzymes than only TesA, the fact that MAFP can synergize with vancomycin, like THL, and that overexpression of TesA can abolish the MAFP synergistic growth inhibition, further highlights that MAFP effect to inhibit mycobacteria growth in synergy with vancomycin can be attributed to TesA inactivation. The fact that the synergy with vancomycin to inhibit *M. bovis* BCG growth has been previously associated with PDIM deficiency [8,25], and that TesA deficient transposon *M. tuberculosis* mutants, were devoid of PDIM, further suggest that MAFP could synergized with vancomycin by impairing the PDIM synthesis through TesA inhibition, as demonstrated in this study, whereas TesA overexpression counteracted this observed vancomycin susceptibility.

In conclusion, our study presents the biochemical characterization of recombinant TesA TE/esterase activity and the identification of a new inhibitor MAFP, irreversibly binding to the TesA catalytic Ser104 residue. We observed that MAFP increases the susceptibility to vancomycin, potentially by inhibiting TesA involved in PDIM biosynthesis. Although MAFP is too toxic to be considered in the treatment of human infection [31], our finding opens an additional new route for further development of anti-TB drug candidates.

Acknowledgment

This work was partially supported by the China Scholarship Council (CSC) (No. 201408210159).

Author contributions

VF, GV, PS equally contributed. VF, GV and PS conceived and supervised the research; AW and VF developed initial concepts; AW, GV, VF, PS, DV, DY designed the experiments; DY, GV, DE, RA, MSK, SZ, MP, GB performed the research; DY, GV, DV, AW, MP, PS, VF analyzed the data; DY drafted the manuscript; GV, GB, JFC, SC, MP, PS and VF revised the manuscript; SC and JFC provided materials; VF obtained funding.

References

- 1 WHO (2018) Global Tuberculosis Report 2018. World Health Organization, Geneva, Switzerland.
- 2 Daffe M, Crick DC and Jackson M (2014) Genetics of capsular polysaccharides and cell envelope (Glyco) lipids. *Microbiol Spectr* **2**, 14.
- 3 Gopal P, Yee M, Sarathy J, Low JL, Sarathy JP, Kaya F, Dartois V, Gengenbacher M and Dick T (2016) Pyrazinamide resistance is caused by two distinct mechanisms: prevention of coenzyme A depletion and loss of virulence factor synthesis. *ACS Infect Dis* **2**, 616–626.
- 4 Chavadi SS, Edupuganti UR, Vergnolle O, Fatima I, Singh SM, Soll CE and Quadri LE (2011) Inactivation of *tesA* reduces cell wall lipid production and increases drug susceptibility in mycobacteria. *J Biol Chem* **286**, 24616–24625.
- 5 Bailo R, Bhatt A and Ainsa JA (2015) Lipid transport in *Mycobacterium tuberculosis* and its implications in virulence and drug development. *Biochem Pharmacol* **96**, 159–167.
- 6 Mohandas P, Budell WC, Mueller E, Au A, Bythrow GV and Quadri LE (2016) Pleiotropic consequences of gene knockouts in the phthiocerol dimycocerosate and phenolic glycolipid biosynthetic gene cluster of the opportunistic human pathogen *Mycobacterium marinum*. *FEMS Microbiol Lett* **363**, fnw016.
- 7 Astarie-Dequeker C, Le Guyader L, Malaga W, Seaphanh FK, Chalut C, Lopez A and Guilhot C (2009) Phthiocerol dimycocerosates of *M. tuberculosis* participate in macrophage invasion by inducing changes in the organization of plasma membrane lipids. *PLoS Pathog* **5**, e1000289.
- 8 Soetaert K, Rens C, Wang XM, De Bruyn J, Laneelle MA, Laval F, Lemassu A, Daffe M, Bifani P, Fontaine V *et al.* (2015) Increased vancomycin susceptibility in mycobacteria: a new approach to identify synergistic activity against multidrug-resistant mycobacteria. *Antimicrob Agents Chemother* **59**, 5057–5060.
- 9 Alibaud L, Rombouts Y, Trivelli X, Burguiere A, Cirillo SL, Cirillo JD, Dubremetz JF, Guerardel Y, Lutfalla G and Kremer L (2011) A *Mycobacterium marinum* TesA mutant defective for major cell wall-associated lipids is highly attenuated in *Dictyostelium discoideum* and zebrafish embryos. *Mol Microbiol* **80**, 919–934.
- 10 Arbues A, Malaga W, Constant P, Guilhot C, Prandi J and Astarie-Dequeker C (2016) Trisaccharides of phenolic glycolipids confer advantages to pathogenic mycobacteria through manipulation of host-cell pattern-recognition receptors. *ACS Chem Biol* **11**, 2865–2875.
- 11 Reed MB, Domenech P, Manca C, Su H, Barczak AK, Kreiswirth BN, Kaplan G and Barry CE 3rd (2004) A glycolipid of hypervirulent tuberculosis strains that inhibits the innate immune response. *Nature* **431**, 84–87.
- 12 Camacho LR, Ensergueix D, Perez E, Gicquel B and Guilhot C (1999) Identification of a virulence gene cluster of *Mycobacterium tuberculosis* by signature-tagged transposon mutagenesis. *Mol Microbiol* **34**, 257–267.
- 13 Rao A and Ranganathan A (2004) Interaction studies on proteins encoded by the phthiocerol dimycocerosate

- locus of *Mycobacterium tuberculosis*. *Mol Genet Genomics* **272**, 571–579.
- 14 Waddell SJ, Chung GA, Gibson KJ, Everett MJ, Minnikin DE, Besra GS and Butcher PD (2005) Inactivation of polyketide synthase and related genes results in the loss of complex lipids in *Mycobacterium tuberculosis* H37Rv. *Lett Appl Microbiol* **40**, 201–206.
 - 15 Jain M, Petzold CJ, Schelle MW, Leavell MD, Mougous JD, Bertozzi CR, Leary JA and Cox JS (2007) Lipidomics reveals control of *Mycobacterium tuberculosis* virulence lipids via metabolic coupling. *Proc Natl Acad Sci USA* **104**, 5133–5138.
 - 16 Kotowska M and Pawlik K (2014) Roles of type II thioesterases and their application for secondary metabolite yield improvement. *Appl Microbiol Biotechnol* **98**, 7735–7746.
 - 17 Nguyen PC, Nguyen VS, Martin BP, Fourquet P, Camoin L, Spilling CD, Cavalier JF, Cambillau C and Canaan S (2018) Biochemical and structural characterization of TesA, a Major Thioesterase required for outer-envelope lipid biosynthesis in *Mycobacterium tuberculosis*. *J Mol Biol* **430**, 5120–5136.
 - 18 Gu S, Chen J, Dobos KM, Bradbury EM, Belisle JT and Chen X (2003) Comprehensive proteomic profiling of the membrane constituents of a *Mycobacterium tuberculosis* strain. *Mol Cell Proteomics* **2**, 1284–1296.
 - 19 Jain M and Cox JS (2005) Interaction between polyketide synthase and transporter suggests coupled synthesis and export of virulence lipid in *M. tuberculosis*. *PLoS Pathog* **1**, e2.
 - 20 Riddles PW, Blakeley RL and Zerner B (1983) Reassessment of Ellman's reagent. *Methods Enzymol* **91**, 49–60.
 - 21 Hunt MC, Solaas K, Kase BF and Alexson SE (2002) Characterization of an acyl-coA thioesterase that functions as a major regulator of peroxisomal lipid metabolism. *J Biol Chem* **277**, 1128–1138.
 - 22 Delorme V, Dhoub R, Canaan S, Fotiadu F, Carriere F and Cavalier JF (2011) Effects of surfactants on lipase structure, activity, and inhibition. *Pharm Res* **28**, 1831–1842.
 - 23 Nguyen PC, Delorme V, Benarouche A, Martin BP, Paudel R, Gnawali GR, Madani A, Puppo R, Landry V, Kremer L et al. (2017) Cyclopostins and Cyclophostin analogs as promising compounds in the fight against tuberculosis. *Sci Rep* **7**, 11751.
 - 24 Goude R, Roberts DM and Parish T (2015) Electroporation of mycobacteria. *Methods Mol Biol* **1285**, 117–130.
 - 25 Rens C, Laval F, Daffe M, Denis O, Frita R, Baulard A, Wattiez R, Lefevre P and Fontaine V (2016) Effects of Lipid-lowering drugs on vancomycin susceptibility of mycobacteria. *Antimicrob Agents Chemother* **60**, 6193–6199.
 - 26 Sastry GM, Adzhigirey M, Day T, Annabhimoju R and Sherman W (2013) Protein and ligand preparation: parameters, protocols, and influence on virtual screening enrichments. *J Comput Aided Mol Des* **27**, 221–234.
 - 27 Friesner RA, Murphy RB, Repasky MP, Frye LL, Greenwood JR, Halgren TA, Sanschagrin PC and Mainz DT (2006) Extra precision glide: docking and scoring incorporating a model of hydrophobic enclosure for protein-ligand complexes. *J Med Chem* **49**, 6177–6196.
 - 28 Arai K, Ishimitsu T, Fushinobu S, Uchikoba H, Matsuzawa H and Taguchi H (2010) Active and inactive state structures of unliganded Lactobacillus casei allosteric L-lactate dehydrogenase. *Proteins* **78**, 681–694.
 - 29 Goldsmith EJ, Sprang SR, Hamlin R, Xuong NH and Fletterick RJ (1989) Domain separation in the activation of glycogen phosphorylase a. *Science* **245**, 528–532.
 - 30 Ravindran MS, Rao SP, Cheng X, Shukla A, Cazenave-Gassiot A, Yao SQ and Wenk MR (2014) Targeting lipid esterases in mycobacteria grown under different physiological conditions using activity-based profiling with tetrahydrolipstatin (THL). *Mol Cell Proteomics* **13**, 435–448.
 - 31 Li H, Schopfer LM, Nachon F, Froment MT, Masson P and Lockridge O (2007) Aging pathways for organophosphate-inhibited human butyrylcholinesterase, including novel pathways for isomalathion, resolved by mass spectrometry. *Toxicol Sci* **100**, 136–145.
 - 32 Amara S, Delorme V, Record M and Carriere F (2012) Inhibition of phospholipase A1, lipase and galactolipase activities of pancreatic lipase-related protein 2 by methyl arachidonyl fluorophosphonate (MAFP). *Biochim Biophys Acta* **1821**, 1379–1385.
 - 33 Berge RK, Slinde E and Farstad M (1980) Discontinuities in Arrhenius plots due to formation of mixed micelles and change in enzyme substrate availability. *FEBS Lett* **109**, 194–196.
 - 34 Berge RK, Slinde E and Farstad M (1981) Variations in the activity of microsomal palmitoyl-CoA hydrolase in mixed micelle solutions of palmitoyl-CoA and non-ionic detergents of the triton X series. *Biochim Biophys Acta* **666**, 25–35.
 - 35 Berge RK and Farstad M (1979) Purification and characterization of long-chain acyl-CoA hydrolase from rat liver mitochondria. *Eur J Biochem* **96**, 393–401.
 - 36 Wang F, Langley R, Gulten G, Wang L and Sacchettini JC (2007) Identification of a type III thioesterase reveals the function of an operon crucial for Mtb virulence. *Chem Biol* **14**, 543–551.
 - 37 Goins CM, Sudasinghe TD, Liu X, Wang Y, O'Doherty GA and Ronning DR (2018) Characterization of Tetrahydrolipstatin and Stereoderivatives on the Inhibition of Essential

- Mycobacterium tuberculosis* Lipid Esterases. *Biochemistry* **57**, 2383–2393.
- 38 Parker SK, Barkley RM, Rino JG and Vasil ML (2009) *Mycobacterium tuberculosis* Rv3802c encodes a phospholipase/thioesterase and is inhibited by the antimycobacterial agent tetrahydrolipstatin. *PLoS ONE* **4**, e4281.
- 39 Seeliger JC, Holsclaw CM, Schelle MW, Botyanszki Z, Gilmore SA, Tully SE, Niederweis M, Cravatt BF, Leary JA and Bertozzi CR (2012) Elucidation and chemical modulation of sulfolipid-1 biosynthesis in *Mycobacterium tuberculosis*. *J Biol Chem* **287**, 7990–8000.
- 40 Ritchie MK, Johnson LC, Clodfelter JE, Pemble CWT, Fulp BE, Furdui CM, Kridel SJ and Lowther WT (2016) Crystal structure and substrate specificity of human thioesterase 2: insights into the molecular basis for the modulation of fatty acid synthase. *J Biol Chem* **291**, 3520–3530.
- 41 Fako VE, Zhang JT and Liu JY (2014) Mechanism of orlistat hydrolysis by the thioesterase of human fatty acid synthase. *ACS Catal* **4**, 3444–3453.
- 42 Hadvary P, Sidler W, Meister W, Vetter W and Wolfer H (1991) The lipase inhibitor tetrahydrolipstatin binds covalently to the putative active site serine of pancreatic lipase. *J Biol Chem* **266**, 2021–2027.
- 43 Pemble CWT, Johnson LC, Kridel SJ and Lowther WT (2007) Crystal structure of the thioesterase domain of human fatty acid synthase inhibited by Orlistat. *Nat Struct Mol Biol* **14**, 704–709.
- 44 Huang Z, Payette P, Abdullah K, Cromlish WA and Kennedy BP (1996) Functional identification of the active-site nucleophile of the human 85-kDa cytosolic phospholipase A2. *Biochemistry* **35**, 3712–3721.
- 45 Casida JE and Quistad GB (2005) Serine hydrolase targets of organophosphorus toxicants. *Chem Biol Interact* **157–158**, 277–283.
- 46 Yang LL, Yang X, Li GB, Fan KG, Yin PF and Chen XG (2016) An integrated molecular docking and rescoring method for predicting the sensitivity spectrum of various serine hydrolases to organophosphorus pesticides. *J Sci Food Agric* **96**, 2184–2192.
- 47 Petrikovics I, Wales M, Budai M, Yu JC and Szilasi M (2012) Nano-intercalated organophosphorus-hydrolyzing enzymes in organophosphorus antagonism. *AAPS PharmSciTech* **13**, 112–117.
- 48 Tallman KR, Levine SR and Beatty KE (2016) Small-molecule probes reveal esterases with persistent activity in dormant and reactivating *Mycobacterium tuberculosis*. *ACS Infect Dis* **2**, 936–944.
- 49 Aloulou A, Rodriguez JA, Fernandez S, van Oosterhout D, Puccinelli D and Carriere F (2006) Exploring the specific features of interfacial enzymology based on lipase studies. *Biochim Biophys Acta* **1761**, 995–1013.

Supporting information

Additional supporting information may be found online in the Supporting Information section at the end of the article.

Fig. S1. Chemical structures.

Fig. S2. Recombinant TesA N-terminal sequence, TesA quality and thermal stability determination.

Fig. S3. Thioesterase activity assay in the presence of Triton X-100.

Fig. S4. Microsequencing of the TesA peptide ‘IDDP-VAFFGHSMGGMLAFEVALR’ in the *m/z* range 0–2000.

Fig. S5. Superposition of the best score binding pose of propylphosphate onto the crystal position of truncated CyC₁₇.

Fig. S6. Binding mode of MAFP in the dimer featuring a binding mode of palmitoyl-CoA in one of the two binding sites.

Fig. S7. Model of TesA conformational changes during catalysis with different substrates or MAFP.